Molecular characterization of the missing electron pathways for butanol synthesis in Clostridium acetobutylicum

Celine Foulquier
University of Toulouse
Anntoine Rivière
University of Toulouse
Mathieu Heulot
University of Toulouse
Suzana Dos Reis
Institut de Pharmacologie et de Biologie Structurale, IPBS, Université de Toulouse, CNRS, UPS, Toulouse
Caroline Perdu
University of Toulouse
Laurence Girbal
University of Toulouse
Mailys Pinault
University of Toulouse
Simon Dusséaux
University of Toulouse
Philippe Soucaille (soucaille@insa-toulouse.fr)
University of Toulouse https://orcid.org/0000-0002-1724-7136
Isabelle Meynial-Salles
Université de Toulouse, INSA, UPS, INP, LISBP, INRA UMR792, CNRS UMR5504, Toulouse

Article

Keywords: electron pathways, metabolic engineering, butanol

Posted Date: September 16th, 2021

DOI: https://doi.org/10.21203/rs.3.rs-882149/v1

Version of Record: A version of this preprint was published at Nature Communications on August 10th, 2022. See the published version at https://doi.org/10.1038/s41467-022-32269-1.

Molecular characterization of the missing electron pathways for butanol synthesis in *Clostridium acetobutylicum*

Céline Foulquier[1†], Antoine Rivière[1†], Mathieu Heulot[1], Suzanna Dos Reis[1], Caroline Perdu[1], Laurence Girbal[1], Mailys Pinault[1], Simon Dusséaux[1], Philippe Soucaille[1, 2*] & Isabelle Meynial-Salles[1]

[†] Céline Foulquier and Antoine Rivière contributed equally to this work.

1 TBI, Université de Toulouse, CNRS, INRAE, INSA, Toulouse, France

2 BBSRC/EPSRC Synthetic Biology Research Centre, School of Life Sciences, Centre for Biomolecular Sciences, University of Nottingham, United Kingdom

*Corresponding author: correspondence and material requests should be addressed to soucaille@insa-toulouse.fr

Abstract:

Clostridium acetobutylicum is a promising biocatalyst for the production of n-butanol at high yield from renewable resources. Several metabolic strategies have already been developed to increase butanol yields, most often based on carbon pathway redirection. However, it was previously demonstrated that the activities of both ferredoxin-$NADP^+$ reductase and ferredoxin-NAD^+ reductase, whose encoding genes remained unknown until this study, were necessary to produce the NADPH and the extra NADH needed for butanol synthesis under solventogenic conditions. Here, we purified, identified and characterized the proteins responsible for both ferredoxin-$NADP^+$ reductase and ferredoxin-NAD^+ reductase activities and demonstrated the involvement of the identified enzymes in butanol synthesis through a reverse genetic approach. We further demonstrated the yield of butanol formation was limited by the level of expression of *CAC_0764,* the ferredoxin-$NADP^+$ reductase encoding gene.

The integration of these enzymes into metabolic engineering strategies introduces new opportunities for developing a homobutanologenic *C. acetobutylicum* strain.

Introduction:

Clostridium acetobutylicum is a gram-positive, spore-forming anaerobic bacterium capable of converting various sugars and polysaccharides to organic acids (acetate and butyrate) and solvents (acetone, butanol, and ethanol). Due to its importance in the industrial production of the bulk chemicals acetone and butanol (1–3) and its potential use in the production of n-butanol, a promising biobased liquid fuel with several advantages over ethanol (4-5), much research has focused on i) understanding the regulation of solvent formation (6–15) and ii) metabolically engineering this microorganism to produce high yields of alcohols (16–18).

Using a global system biology approach to the characterization of the solventogenic metabolism of a phosphate-limited chemostat culture of *C. acetobutylicum,* the six steps involved in the conversion of acetyl-CoA to butanol (Fig. 1) were fully characterized (19): the main enzyme responsible for crotonyl-CoA reduction to butyryl-CoA is the BCD complex (encoded by *bcd*, *etfA* and *etfB*), a bifurcating enzyme consuming 2 moles of NADH and producing one mole of reduced ferredoxin, and the last two steps of butanol production are catalyzed by AdhE1 through its NADH-dependent aldehyde dehydrogenase activity and by BdhB, BdhC and BdhA through their NADPH-dependent butanol dehydrogenase activity. These results have a strong impact on electron flux distribution, as it was demonstrated that both ferredoxin $NADP^+$ reductase and ferredoxin NAD^+ reductase activities were necessary to produce the NADPH and the extra NADH needed for butanol synthesis from acetyl-CoA (Fig. 2)(19). Although the activities of these enzymes were previously detected in *C. acetobutylicum* (6, 20), the encoding genes remained unknown (19, 21). Ferredoxin-$NADP^+$ reductase enzymes (FNOR) (EC 1.18.1.3) are distributed over a variety of aerobic organisms from prokaryotes to eukaryotes, especially in plants (22), but have never been purified and characterized from any clostridial species. In contrast, ferredoxin-dependent NAD^+ reduction coupled to proton

export (Rnf) and ferredoxin-dependent transhydrogenases (Nfn) are of central importance in anaerobic bacteria, as they catalyze electron transfer from reduced ferredoxin to $NAD(P)^+$ to maintain the redox balance. Although Rnf and Nfn have been characterized from a molecular perspective in several clostridial species, no homologs have been found in *C. acetobutylicum* (23–25). Moreover, *C. acetobutylicum* cannot produce NADPH by the oxidative pentose-phosphate pathway, as *zwf*, which encodes glucose-6-P dehydrogenase, the first and key enzyme of this pathway, is missing (19, 26).

The aim of this study was to purify and identify the proteins responsible for the ferredoxin-NAD^+ and ferredoxin-$NADP^+$ reductase activities in *C. acetobutylicum* under solventogenic conditions. We further confirmed their essential physiological role in butanol synthesis in *C. acetobutylicum* and demonstrated that butanol production is limited by the electron flux between reduced ferredoxin and both $NADP^+$ and NAD^+.

Results:

Solventogenesis in *C. acetobutylicum*: biochemical analysis of the glucose to n-butanol pathway:

C. acetobutylicum can in theory convert one mole of glucose into one mole of n-butanol. The conversion of one mole of glucose to 2 moles of acetyl-CoA is associated with the production of 2 moles of NADH in the EMP pathway and 2 moles of reduced ferredoxin during the decarboxylation of 2 moles of pyruvate to 2 acetyl-CoA using pyruvate ferredoxin oxidoreductase (PFOR) (Fig. 1). However, under solventogenic conditions, the conversion of 2 moles of acetyl-CoA to one mole of n-butanol produces one mole of reduced ferredoxin during the reduction of crotonyl-CoA to butyryl-CoA by butyryl-CoA dehydrogenase (BCD) and

consumes 4 moles of NADH and one mole of NADPH to reduce butyraldehyde to n-butanol (Fig. 1) by the NADPH-dependent alcohol dehydrogenases BdhB, BdhC and BdhA (19).

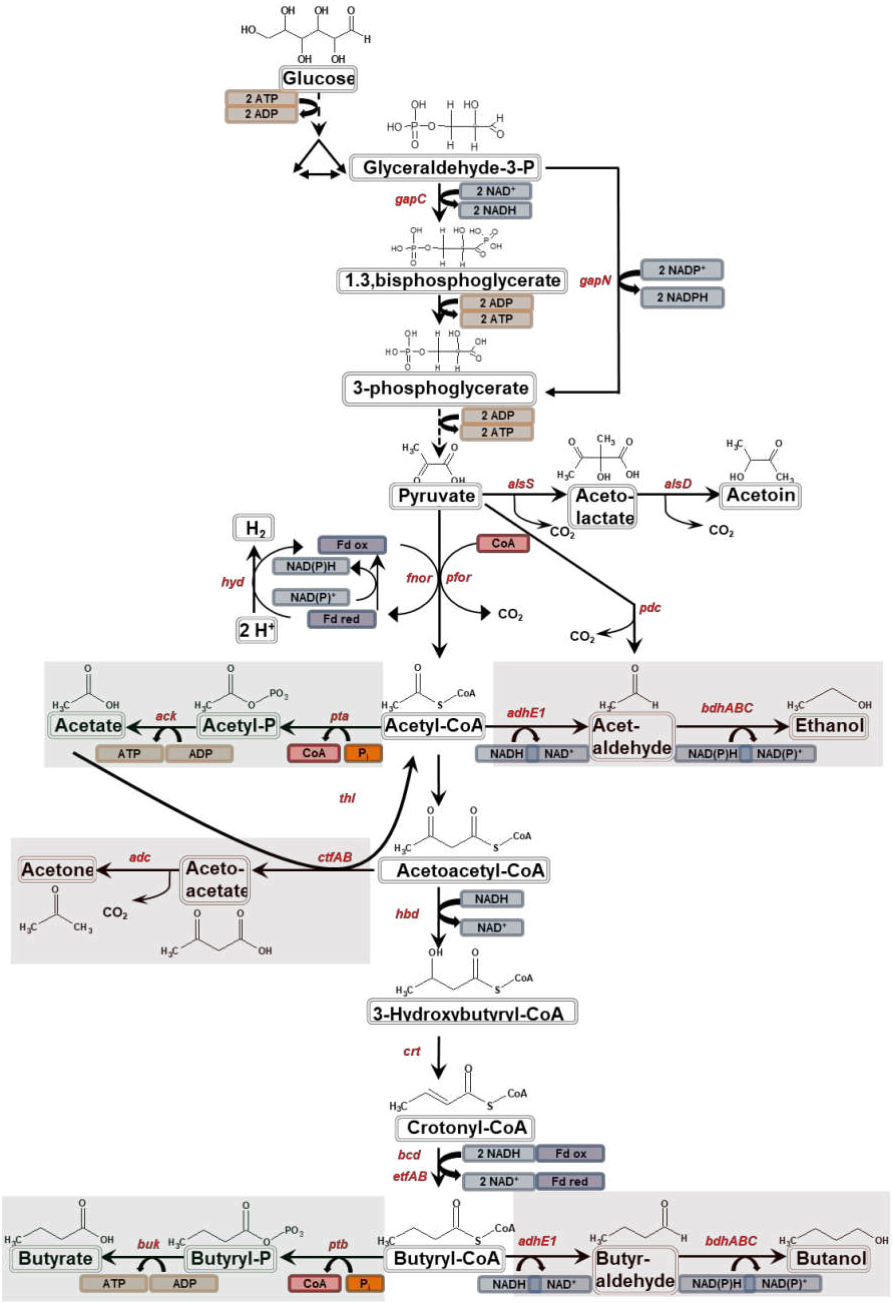

Fig. 1 Central metabolism of *Clostridium acetobutylicum*. The green box indicates the primary products under acidogenic conditions, whereas the red box indicates the primary products under solventogenic conditions. The letters in red and italics indicate the corresponding genes. Abbreviations: *ack*, acetate kinase; *adc*, acetoacetate decarboxylase; *adhE1*, aldehyde dehydrogenase; *adhE2*, bifunctional aldehyde/alcohol dehydrogenase; *alsD*, alpha-acetolactate decarboxylase; *alsS*, acetolactate synthase; *bcd*, butyryl-CoA dehydrogenase; *bdh*, butanol dehydrogenase; *buk*, butyrate kinase; *crt*, crotonase; *ctfAB*, CoA-transferase; *etf*,

electron transfer flavoprotein; *hbd*, 3-hydroxybutyryl-CoA dehydrogenase; *hyd*, hydrogenase; *fnor*, ferredoxin-NAD(P)$^+$ oxidoreductase; *pdc*, pyruvate decarboxylase; *pfor*, pyruvate:ferredoxin oxidoreductase; *pta*, phosphotransacetylase; *ptb*, phosphotransbutyrylase; *thl*, thiolase; *gapC*, NADH-dependent glyceraldehyde-3-phosphate dehydrogenase; *gapN*, nonphosphorylating NADPH-producing glyceraldehyde-3-phosphate dehydrogenase; Fd ox represents oxidized ferredoxin, whereas Fd red represents reduced ferredoxin.

As the EMP pathway produces less NADH than the n-butanol pathway consumes, for each mole of n-butanol produced, 2 moles of reduced ferredoxin must be used to produce two moles of NADH using a ferredoxin-NAD$^+$ reductase. Furthermore, as *C. acetobutylicum* does not have an oxidative pentose-phosphate pathway (26) and as the nonphosphorylating NADPH producing glyceraldehyde-3-P dehydrogenase encoded by *gapN* is expressed at a low level (19), for each mole of n-butanol produced, one mole of reduced ferredoxin must also be used to produce one mole of NADPH using a ferredoxin-NADP$^+$ reductase.

From this analysis, it is clear that ferredoxin-NAD$^+$ and ferredoxin-NADP$^+$ reductases are key to providing electrons for the production of n-butanol (Fig. 2), but until now, the proteins involved remained totally unknown. It was therefore decided to purify all the enzymes with ferredoxin-NAD$^+$ or ferredoxin-NADP$^+$ reductase activity.

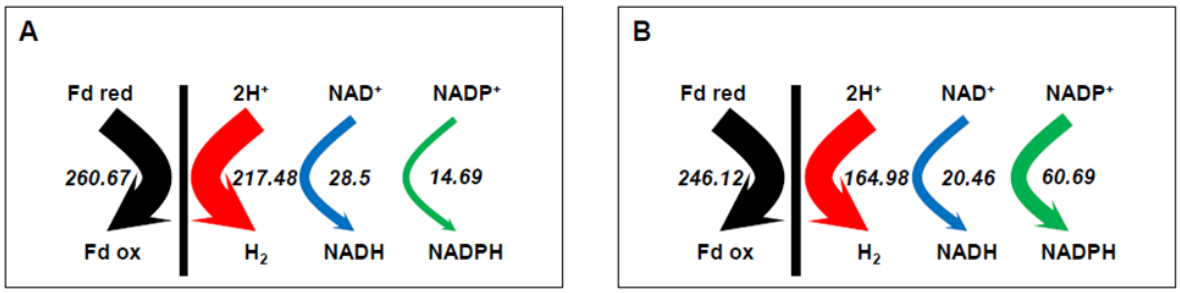

Fig. 2. Metabolic flux analysis of *C. acetobutylicum* in phosphate limited chemostat cultures under acidogenic (pH 6.3) (A) and solventogenic (pH 4.4) (B) conditions. All values (mmol/gDCW/h) are normalized to the flux of glucose consumption (19).

Purification and characterization of the ferredoxin-NADP$^+$ reductase of *C. acetobutylicum:*

Proteins with ferredoxin-NADP$^+$ reductase activities were purified under strict anaerobic conditions from *C. acetobutylicum* ATCC 824 crude extract as described in the methods. Proteins were first captured using a Capto DEAE matrix, and active eluted fractions were pooled and then purified using a ResourceQ column. After concentration, active eluted fractions were finally loaded onto a Superose 12 column. The results of a traditional purification are presented in Table 1. Activities were measured at 340 nm by NADP$^+$ reduction using CAC0303 reduced ferredoxin as the electron donor. During the purification process, the purified enzyme lost 60% of its activity after 48 hours.

Table 1 Purification of Ferredoxin NADP$^+$ reductases from *C. acetobutylicum*

Steps	Activity (Units)	Protein (mg)	Specific activity (units/mg)	Recovery (%)	Purification fold
Crude extract	2.7	150	0.02	100	1
Streptomycin sulfate supernatant	2.46	104	0.02	92	1.33
CAPTO DEAE column	0.52	1.93	0.27	20	15
Resource Q column	0.066	0.22	0.3	2.44	12.5
Superose 12 column	0.02	0.012	1.73	0.74	96

Active eluted fractions from gel filtration were then subjected to denaturing gel electrophoresis. As shown in Supplementary Fig. 1, the increase in ferredoxin-NADP$^+$ reductase activity seems to be linked to the concentration of a protein with an apparent molecular mass of 45 kDa on SDS-PAGE.

The region of the gel corresponding to this protein was eluted, digested by trypsin and analyzed by nano-LC–MS/MS as described in the methods. The encoding gene is *CA_C0764,* annotated as an NADPH-dependent glutamate synthase beta subunit. Identical treatments were applied to the 40 and 55 kDa proteins, which were identified as thiolase (*CA_C2873*) and phosphoribosylaminoimidazole carboxamide formyltransferase-IMP cyclohydrolase

(*CA_C1395*). None of these proteins are oxidoreductases. The gene identification results were used to extract the quantitative transcriptomic and proteomic data performed by Yoo *et al.*, and it was confirmed that the expression of *CA_C0764* from a monocistronic operon was higher under solventogenic condition than under acidogenic condition (Fig. 3).

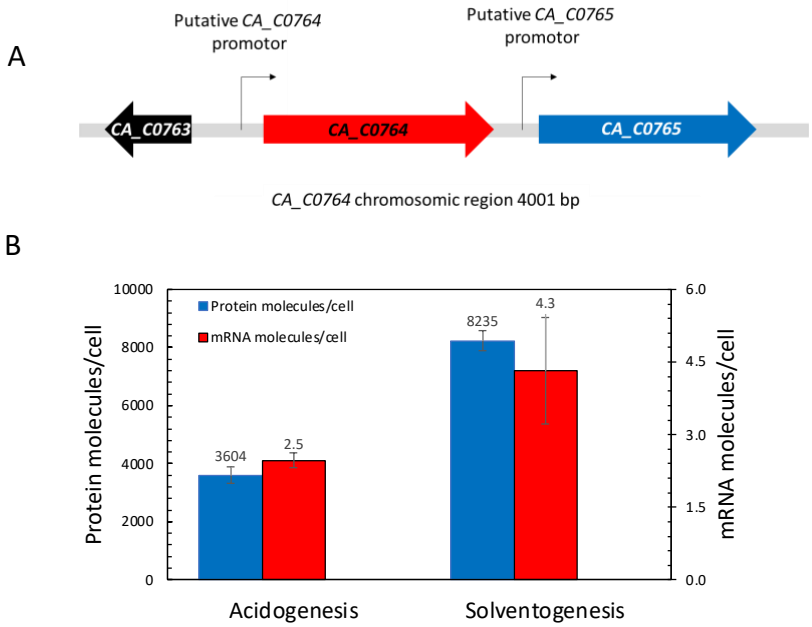

Fig. 3: A: *CA_C0764* chromosomic region of *C. acetobutylicum.* Putative -35 and -10 sequences of *CA_C0764* and *CA_C0765* were analyzed by the BPROM tool. B: Analysis of *CA_C0764* expression under acidogenesis and solventogenesis (19).

To validate the ferredoxin-NADP$^+$ reductase activity of the CAC0764 protein, the *CA_C0764* gene was cloned into a replicative plasmid to be fused with a small tag (Strep-tag II) placed in the C-terminal position of CAC0764, as described in Methods. The recombinant protein was homologously overexpressed in MGC*Δcac1502* and then purified from the crude extract in a single step using affinity chromatography on a Strep-Tactin column. Recombinant proteins were eluted with desthiobiotin, and the purity of the eluted fraction was checked by SDS-PAGE with Coomassie blue staining (Supplementary Fig. 2).

As expected, denaturing gel electrophoresis showed a single band in the eluted fraction corresponding to an apparent molecular mass of 45 kDa, demonstrating that CAC0764 was pure.

In vitro ferredoxin NAD(P)$^+$ reductase and NAD(P)H ferredoxin reductase activities were evaluated in the recovered pure fraction using NADP$^+$ reduction with reduced ferredoxin as an electron donor or methyl viologen reduction by NADPH. According to Supplementary Fig. 2, purified CAC0764-Strep-tag II exhibited both NAPDH ferredoxin reductase and ferredoxin-NADP$^+$ reductase activities, and neither activity was observed in the presence of NADH and NAD$^+$. These results confirmed that CAC0764 is an FNOR enzyme that is strictly NADPH/NADP$^+$ dependent.

Purification and characterization of the ferredoxin-NAD$^+$ reductase of *C. acetobutylicum:*

Proteins with ferredoxin-NAD$^+$ reductase activities were purified under strict anaerobic conditions from *C. acetobutylicum* ATCC 824 crude extract as described in the methods. Proteins were first captured using a Capto DEAE matrix and eluted with a linear gradient of NaCl from 0.1 to 0.25 M, yielding two peaks (one minor and one major) of ferredoxin-NAD$^+$ reductase activities. The peak-activity eluted fractions were pooled separately and then concentrated before being finally loaded onto a Superose 12 or a Resource Q column. The results are presented in Table 2.

Table 2: purification of Ferredoxin NAD$^+$ reductases from *C. acetobutylicum*

Steps		Activity (Units)	Protein (mg)	Specific activity (units/mg)	Recovery (%)	Purification fold
Crude extract		13.4	203	0.07	100	0
Streptomycin sulfate supernatant		9.02	102	0.09	67	1.28
CAPTO DEAE column	major peak 1	7.3	5.44	1.34	54	19.14
	minor peak 2	1.27	4,06	0.31	9.5	4.49
Peak 1 on Superose 12 column		3.43	1.5	2.29	25	32.7
Peak 2 on Resource Q column		0.56	1.5	0.40	4.2	5.71

Active eluted fractions from gel filtration and Resource Q were then loaded onto denaturing gel electrophoresis. As shown in Supplementary Fig. 3, ferredoxin-NAD^+ reductase activity from gel filtration was associated with the presence of 3 proteins of 41, 37, and 34 kDa, and ferredoxin-NAD^+ reductase activity from Resource Q was linked to the presence of two proteins of 167 and 53 kDa. All proteins were eluted, digested by trypsin and analyzed by nano-LC–MS/MS as described in Methods. The results indicated that the three proteins eluted from gel filtration were the three subunits of butyryl-CoA dehydrogenase encoded by *bcd*, *etfB* and etfA, and the two proteins eluted from ResourceQ were the two subunits of NADH-dependent glutamate synthase encoded by *gltA* and *gltB*. The BCD enzyme complex was previously shown to have NADH-ferredoxin reductase activity in the presence of crotonyl-CoA (19). This study shows clearly that BCD also has ferredoxin-NAD^+ reductase activity in the absence of crotonyl-CoA or butyryl-CoA.

To determine if ferredoxin-NAD^+ reductase activity could be obtained in the absence of Bcd, the *etfb-etfa* genes were cloned on a replicative plasmid with a sequence encoding Strep-tag II placed in the 3' position of *etfB* with and without *bcd* as the first gene of the synthetic operon, as described in Yoo *et al*. 2015. The recombinant proteins were produced in *E. coli* from the two plasmids and then purified on a Strep-Tactin column. When all three genes were expressed, an active complex could be purified, while when only two genes were expressed, only EtfB could be purified, indicating that EtfB and EtfA cannot form a complex in the absence of Bcd.

The ferredoxin-NAD^+ reductase, ferredoxin-$NADP^+$ reductase, NADH-ferredoxin, and NADPH-ferredoxin reductase activities of the Bcd-EtfAB complex were evaluated in the purified active fraction recovered from *C. acetobutylicum*. According to Fig. 4, the purified complex exhibited

ferredoxin-NAD$^+$ reductase activity, but no ferredoxin-NADP$^+$ reductase activity, no NADH-ferredoxin, and no NADPH-ferredoxin reductase activity were detected. These results confirmed that in addition to its butyryl-CoA dehydrogenase activity, the Bcd-EtfA-EtfB complex can exhibit ferredoxin-NAD$^+$ reductase activity in the absence of any CoA derivative.

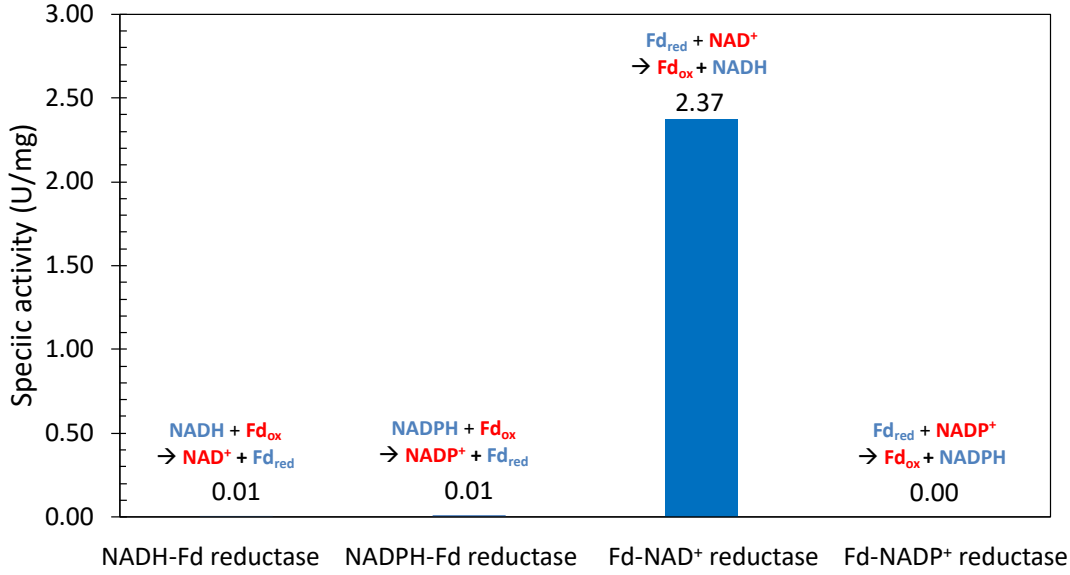

Fig. 4: Enzyme activities of the purified Bcd-EftB-Strep-tag-EtfA complex overexpressed and purified from *C. acetobutylicum* cells.

Finally, the ferredoxin-NAD$^+$ reductase, ferredoxin-NADP$^+$ reductase, NADH-ferredoxin reductase, and NADPH-ferredoxin reductase activities of the GltAB complex were evaluated in the purified active fraction recovered from *C. acetobutylicum*. Both ferredoxin-NAD$^+$ reductase and NADH-ferredoxin reductase activities were detected, while no ferredoxin-NADP$^+$ reductase or NADPH-ferredoxin reductase activity was measured, indicating that GltAB is strictly NADH/NAD$^+$ dependent.

Construction of knockout mutants of the genes encoding enzymes with ferredoxin-NAD$^+$ reductase and ferredoxin-NADP$^+$ reductase activities:

To investigate the role of ferredoxin-NAD(P)$^+$ reductases in the production of butanol *in vivo,* group II intron-based ClosTron technology (27) was used to inactivate the *CA_C0764, gltB* and

etfB genes in *MGCΔcac1502* (28). This technology uses the insertion of a group II intron into a genomic target site coupled to a retrotransposition-activated marker (erythromycin resistance), allowing stable gene inactivation. The retargeted introns were first directed to be inserted at position 407/408 on the sense strand of *CA_C0764* and at position 181/182 on the sense strand of *gltB*. After mutagenesis, the insertion mutants were checked by combining PCR screening, sequencing and Southern hybridization (Fig. 4). Both *MGCΔcac1502-CA_C0764-408s::CT* and *MGCΔcac1502-gltb181s::CT* were successfully constructed.

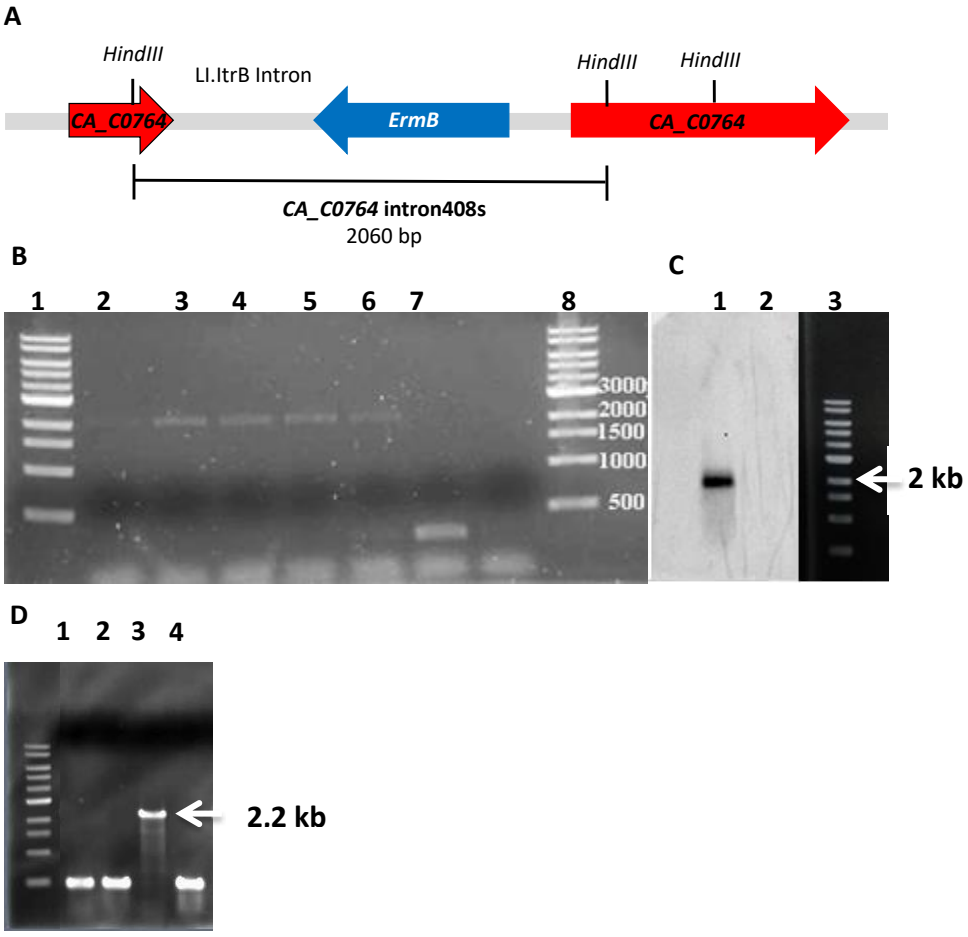

Fig 4: Construction of the *MGCΔcac1502-CA_C0764-408s::CT* and *MGCΔcac1502-gltb181s::CT* mutants: **A**) Schematic representation of the *CA_C0764* gene with a group II intron inserted at position 408 on the sense strand of *CA_C0764.* **B**) PCR screening for the identification of putative *CA_C0764-408s::CT* mutants using gene-specific primers flanking the intron insertion site (lanes 2 to 5) (expected size 2060 bp) and PCR control with wild-type DNA (lane 7) (expected size 270 bp), lanes 1 and 8 DNA

ladder. **C**) Southern hybridization to demonstrate the presence of a single intron insertion in the selected *MGCΔcac1502cac0764-408s::CT* mutant. The intron probe was DIG labeled and hybridized to HindIII-HF digested genomic DNA of the *MGCΔcac1502cac0764-408s::CT* mutant (lane 2) with an expected size of 1970 bp. The HindIII-HF digested genomic DNA of the *C. acetobutylicum MGCΔcac1502* strain (lane 1) was also tested as a negative control. Lane 3 is a 1 kb DNA ladder. **D**) PCR screening for the identification of putative *gltb181s::CT* mutant using gene-specific primers flanking the intron insertion site (lanes 1 to 3) (expected size 2200 bp) and PCR control with wild-type DNA (lane 4) (expected size 500 bp), lane 1 DNA ladder.

A similar approach using the ClosTron method was used to inactivate the *etfB* gene. Despite repeated attempts and the use of at least two different retargeted ClosTron plasmids, insertions into the *etfB* gene could not be obtained. The low number of erythromycin-resistant clones that did arise had apparently inserted elsewhere in the genome, suggesting that the ferredoxin-NAD^+ reductase activity of BCD is essential for *C. acetobutylicum*.

Role of ferredoxin-$NADP^+$ reductase in the central metabolism of *C. acetobutylicum*:

To better understand the role of ferredoxin-$NADP^+$ reductase in the central metabolism of *C. acetobutylicum*, the growth and product formation of a strain with an inactivated *cac0764* gene (*MGC∆cac1502CA_C0764-408s::CT*) and a strain overexpressing *cac0764* (*MGC∆cac1502 (pCLFCA_C0764)*) were compared to the control *MGC∆cac1502* strain and the *MGC∆cac1502 (pCons2-1*) strain containing an empty control plasmid*,* respectively. The final product yields of all strains after 10 days of culture are shown in Fig. 5 A and B:

A

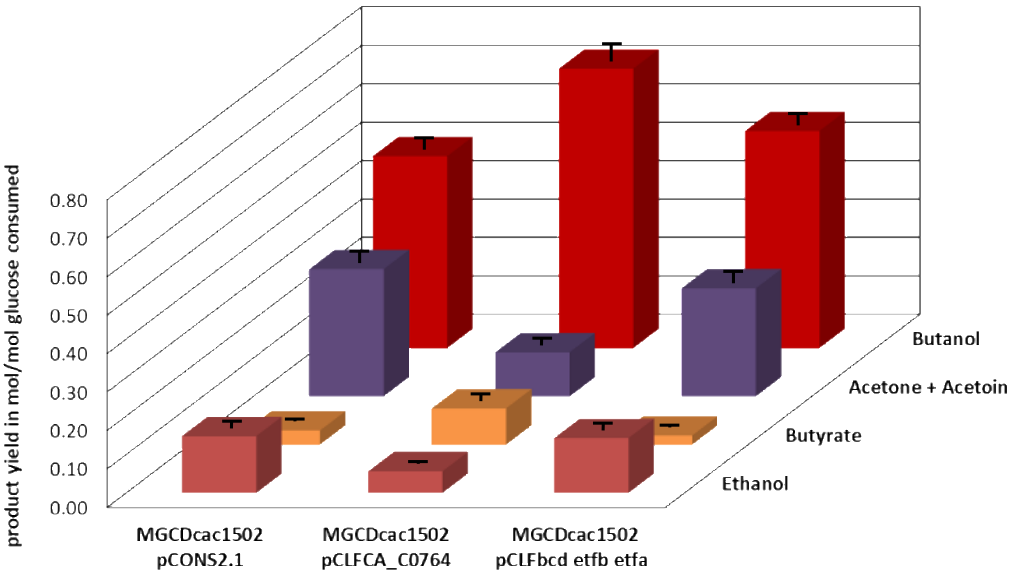

B

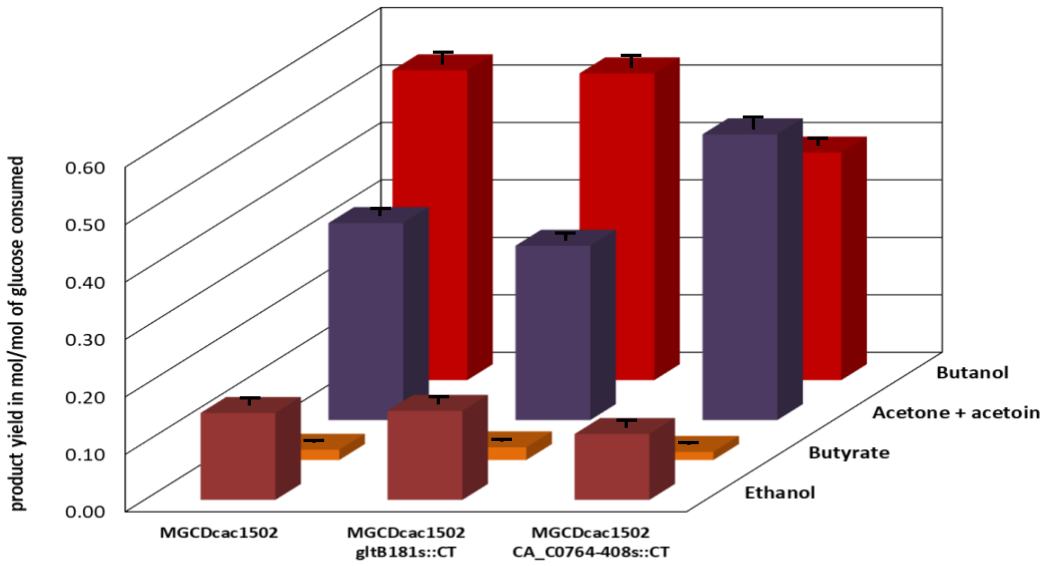

Fig. 5: Comparative final product yields in mol/mol of glucose consumed for all *C. acetobutylicum* strains: **A**) *MGCΔcac1502 (pCons2-1), MGCΔcac1502 (pCLFCA_C0764), MGCΔcac1502 (pCLFbcd-etfb--etfa)* **B***) MGCΔcac1502, MGCΔcac1502-gltB181s:CT, MGCΔcac1502-CA_C0764-408s::CT.* Each error bar indicates the SEM around the mean of three independent cultures.

Fig. 5B shows that the inactivation of the gene encoding the ferredoxin-NADP$^+$ reductase caused a marked decrease in the butanol yield (40% of the theoretical yield) in comparison to the parental *MGCΔcac1502* strain (54% of the theoretical yield). Conversely, the acetone +

acetoin yield was almost doubled (34% of the theoretical yield in the parental *MGC⊿cac1502* strain versus 50% of the theoretical yield when *CA_CO764* was inactivated). On the other hand, the overexpression of the ferredoxin-$NADP^+$ reductase-encoding gene (Fig. 5a) favored butanol production and significantly increased the butanol yield (from 50% to 72% of the theoretical yield) at the expense of acetone + acetoin production, whose yield was strongly reduced from 33% to 11% of the theoretical yield. Finally, the strain with the ferredoxin-$NADP^+$ reductase-encoding gene inactivated could be complemented by the introduction of the *pCLF0764* plasmid overexpressing *CA_C0764,* which restored high butanol production (68% of the theoretical yield) (Supplementary Fig. 4). All these results were confirmed by ferredoxin-$NADP^+$ reductase activity measurements (Fig. 6), which showed negligible ferredoxin-$NADP^+$ reductase activity (<0.001 U/mg) when *CA_0764* was inactivated and high ferredoxin-$NADP^+$ reductase specific activity when *CA_0764* was overexpressed from the *pCLF0764* plasmid (1.54 U/mg +/-0.07, versus 0.0326 U/mg +/- 0.007 for the control).

These results clearly demonstrated the involvement of the ferredoxin-$NADP^+$ reductase enzyme in the butanol production pathway of *C. acetobutylicum* under solventogenic conditions. Moreover, it was also demonstrated that the yield of n-butanol was limited by the level of ferredoxin-$NADP^+$ reductase activity.

Role of each of the two enzymes with ferredoxin-NAD^+ reductase activity in the central metabolism of *C. acetobutylicum*:

To better understand the role of ferredoxin-NAD^+ reductases in the central metabolism of *C. acetobutylicum*, a strain with an inactivated *gltB* gene ***(****MGC⊿cac1502-gltB181s:CT)* and a strain overexpressing the genes encoding the Bcd-EtfB-EtfA complex *(MGC⊿cac1502 (pCLF bcd-etfb-etfa))* were grown anaerobically in liquid flasks containing SM with 60 g/l glucose

under the same conditions, and the growth and product formation were measured. Comparative phenotypic analysis was performed by measuring both glucose consumption and the concentration of fermentation products. Inactivation of *gltB* had no effect on the product profile suggesting that the GltAB enzyme complex plays a minor role in the production of NADH from reduced ferredoxin. In contrast, overexpression of the *bcd-etfb-etfa* operon increased the butanol yield (from 50% to 56% of the theoretical yield) at the expense of acetone + acetoin production, which was reduced from 33% to 28% of the theoretical yield. This plus the fact that a knockout *etfB* mutant is not viable, strongly suggests that the BCD complex is responsible for the ferredoxin-NAD^+ reductase activity in *C. acetobutylicum.*

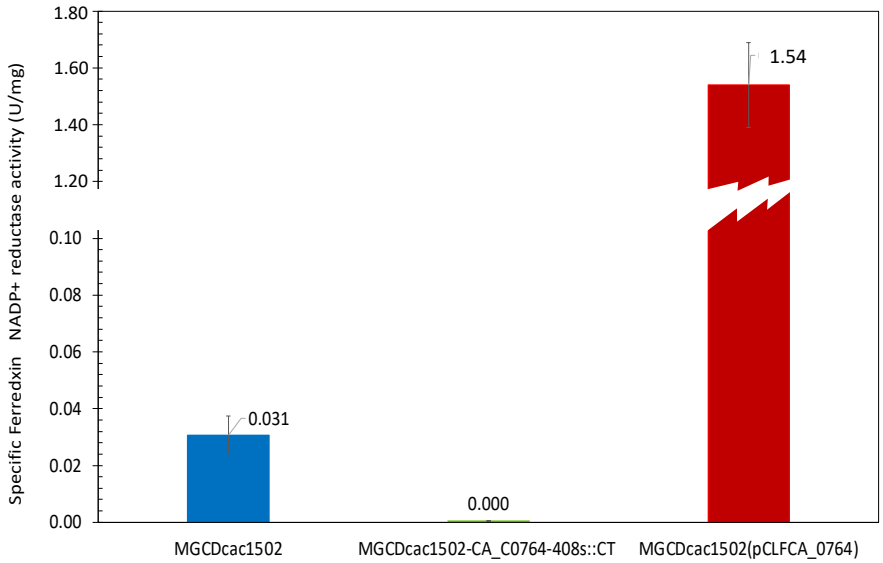

Fig. 6: Specific ferredoxin-$NADP^+$ reductase activity in the cell-free extracts of the MGCΔcac1502 control strain and of both the *MGCΔ1502-CA_C0764-408s::CT* and *MGCΔcac1502(pCLFCA_0764)* mutants. Values are averages from two biological duplicates.

NADPH production in the *MGCΔ1502-CA_C0764-408s::CT mutant*:

In this study, we showed that under solventogenic conditions, CAC0764 is the sole enzyme responsible for ferredoxin-$NADP^+$ reductase activity in *C. acetobutylicum*. As it was previously demonstrated that the oxidative pentose-phosphate pathway is missing in *C. acetobutylicum* (21, 26), we addressed the following question: how can the *MGCΔcac1502-CA_C0764-*

408s::CT mutant generate the NADPH needed for residual butanol production and anabolic reactions? Another NADPH-producing enzyme already identified in *C. acetobutylicum* is glyceraldehyde-3-phosphate dehydrogenase (GapN), encoded by *CA_C3637*, a nonphosphorylating enzyme that catalyzes the oxidation of glyceraldehyde-3-phosphate to 3-phosphoglycerate (Fig. 1). In solventogenic chemostat cultures, this enzyme was shown to catalyze less than 5% of the total flux of the EMP pathway (19). To determine whether *gapN* could be upregulated in the *MGCΔcac1502-CA_C0764-408s::CT* mutant in comparison to the *MGCΔ1502* control strain, quantitative reverse-transcriptase PCR (RT-qPCR) analysis was carried out in both strains to determine the relative expression of the *gapN* and *gapC* (encoding the NADH-dependent GAPDH) genes using the *fabZ* gene as the normalization reference gene (29). Experiments were performed as described in the Materials and Methods, and the normalized fold expression of both *gapN* and *gapC* in both the *MGCΔcac1502* and *MGCΔcac1502-CA_C0764-408s::CT* strains is presented in Fig. 7.

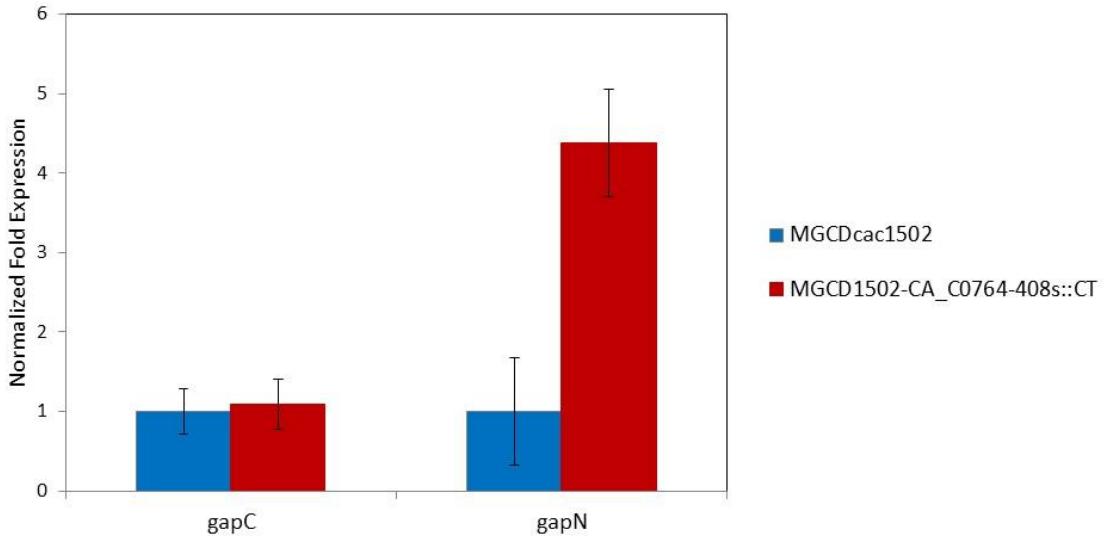

Fig. 7: Normalized fold expression of *gapC and gapN* genes in *MGCΔcac1502-CA_C0764-408s::CT (red).*

According to Fig. 7, the relative expression level of *gapN* in the *MGCΔ1502-CA_C0764-408s::CT* mutant was 4.3-fold higher than the relative expression level of *gapN* in *MGCΔcac1502,* showing that this gene was upregulated in the mutant strain.

Based on the phenotypic analysis performed under solventogenic conditions, the ferredoxin-$NADP^+$ reductase activity determination in the cell crude extract, and the GapN expression results, a redox analysis was performed to determine how reduced ferredoxin is used to achieve the redox balance in each strain (Table 5).

Table 5: Comparative redox analysis of MGC*Δcac1502, MGCΔcac1502-CA_C0764-408s::CT and MGCΔcac1502 pCLFCA-C0764* strains cultured under solventogenic conditions: The distribution of the electrons was described for 1 mole of glucose consumed in the glycolytic pathway.

	STRAINS		
	MGCΔ1502	*MGCΔ1502CA-C0764-408s::CT*	*MGCΔ1502 pCLFcac0764*
moles of NADH produced in the glycolytic pathway	2	1.44	2
moles of NADPH produced in the glycolytic pathway	0	0.56	0
moles of NADH produced from reduced ferredoxin	0.55	0.47	1.6
mole of NADPH produced from reduced ferredoxin	0.74	0	0.8
mole of Fdred reoxidized by hydrogenase	1.2	1.85	0.33

As shown in Table 5, when CAC0764 is inactivated, reduced ferredoxin is mainly used for hydrogen production by HydA hydrogenase, a lower amount is used for NADH production (needed for ethanol, butyrate, lactate and butanol synthesis), and 28% of the EMP flux is catalyzed by GapN to produce the NADPH needed for n-butanol synthesis and anabolism. In contrast, when CAC0764 is overexpressed, reduced ferredoxin is mainly used for the NADH and NADPH formation needed for ethanol, butyrate and butanol production and anabolic reactions.

Discussion:

Ferredoxin-NAD^+ and ferredoxin-$NADP^+$ reductase activities were measured in *C. acetobutylicum* more than 40 years ago (20). Their activities under different physiological conditions were further studied by other groups, but the proteins were never purified and characterized (2,6). Their key role in butanol production was also suggested long ago from a stoichiometric model of the metabolism (30) but never demonstrated using a reverse genetic approach. More recently, using an updated genome-scale model constrained by transcriptomics and proteomics data, Yoo *et al.* in 2015 quantified and demonstrated for the first time the need for both ferredoxin-NAD^+ and ferredoxin-$NADP^+$ reductases to produce butanol under solventogenic conditions. As all the efforts to identify these proteins through blast searches were unsuccessful, a classical purification protocol was developed to isolate both the ferredoxin-NAD^+ and ferredoxin-$NADP^+$ reductases of *C. acetobutylicum*. The applied strategy enabled the identification of only one protein catalyzing ferredoxin-$NADP^+$ reductase activity (encoded by the *CA_C0764* gene) and two enzyme complexes (Bcd-EtfA-EtfB and GltAB) having a ferredoxin-NAD^+ reductase activity.

The ferredoxin-$NADP^+$ reductase from *C. acetobutylicum* does not share any amino acid identity with previously described ferredoxin-$NADP^+$ reductases from other bacteria and shares 30% identity with GltB (the β chain of NADH-dependent glutamate synthase), explaining its incorrect annotation. However, it is expressed as a monocistronic operon, which does not fit with a genetic organization as a bicistronic operon of glutamate synthase-encoding genes. CAC0764 was demonstrated to be strictly NADPH/$NADP^+$ dependent, and FAD is required to retain full enzyme activity, as is generally described for the ferredoxin-$NADP^+$ reductase enzyme family (22).

The two enzyme complexes with NADH-ferredoxin reductase activity BCD and GltAB were previously shown to be a butyryl-CoA dehydrogenase (19), and an NADH dependent glutamate synthase (19) respectively. As the inactivation of *gltB* had no effect on the product profile, the GltAB enzyme complex probably plays a minor role *in vivo* in electrons transfer from reduced ferredoxin to NAD^+. In contrast, the fact that i) overexpression of the *bcd-etfb-etfa* operon increased the butanol yield and ii) a knockout *etfB* mutant is not viable, strongly suggests that the BCD complex is responsible for the ferredoxin-NAD^+ reductase activity in *C. acetobutylicum.* BCD is a bifurcating enzyme reducing crotonyl-CoA to butyryl-CoA with the consumption of two NADHs and the production of one reduced ferredoxin. This allows the endergonic transfer of electrons from NADH to oxidize ferredoxin and eliminate the excess NADH associated with acetate production in acidogenic conditions (6, 19). What is new here is that in the absence of crotonyl-CoA or butyryl-CoA, this enzyme can also carry exergonic electrons transfer from reduced ferredoxin to NAD^+.

From a physiological perspective, inactivation of the ferredoxin-$NADP^+$-encoding gene significantly decreased butanol production and increased acetone production, while its overexpression had the opposite effect, with a very high n-butanol yield from glucose of 72% of the theoretical value. This suggests that butanol production, under solventogenic conditions, is potentially limited by the flux of NADPH production and demonstrates that the carbon fluxes can also be modulated by manipulating the electron fluxes. Furthermore, in the absence of ferredoxin-$NADP^+$ reductase, *C. acetobutylicum* maintains a certain flux of NADPH production by expressing a higher level of *gapN,* a gene coding for nonphosphorylating $NADP^+$-dependent glyceraldehyde-3-P dehydrogenase. In this mutant, up to 28% of the EMP flux is catalyzed by GapN, resulting in lower ATP production.

Attempts to knock out *etfB* to abolish ferredoxin-NAD^+ reductase activity have been unsuccessful. This suggests that *C. acetobutylicum* cannot grow in the absence of ferredoxin-NAD^+ reductase activity. Consistently, all the electron flux analyses performed on chemostat cultures of *C. acetobutylicum* in acidogenic, solventogenic or alcohologenic conditions (19) show a high flux in the reaction catalyzed by ferredoxin-NAD^+ reductase. Furthermore, we can demonstrate using the i965 genome-scale model that an *etfB* mutant that would be unable to produce butyrate and butanol and would have no ferredoxin-NAD^+ reductase activity could survive only if it produced lactate as the only fermentation product. Such a drastic redirection of the metabolic fluxes is probably not possible by regulation of the metabolic pathway and might explain why the *etfB* mutant is not viable.

The discovery of the ferredoxin-$NADP^+$ and ferredoxin-NAD^+ reductase-encoding genes and the demonstration of their key role in butanol production present the possibility of new metabolic engineering strategies to create a homobutanologenic *C. acetobutylicum* strain.

Conclusion:

To the best of our knowledge, these results are the first to be reported on the purification, identification and characterization of the ferredoxin-$NADP^+$ reductase and ferredoxin-NAD^+ reductase of *C. acetobutylicum*. The involvement of the identified enzymes in butanol synthesis under solventogenic conditions was shown.

Methods:

Bacterial strains, plasmids and oligonucleotides:

All bacterial strains, plasmids and oligonucleotides used in or derived from this study are listed in Supplementary Tables 1 and 2.

Culture media and growth conditions:

E. coli strains were grown aerobically at 37°C in Luria-Bertani (LB) medium supplemented, when necessary, with ampicillin (100 μg/mL) and/or chloramphenicol (30 μg/mL). Agar (15 g/L) was added prior to sterilization on LB agar plates.

MGCΔcac1502, *MGCΔcac1502-CA_C0764-408s::CT,* and *MGCΔcac1502 gltB181s::CT* strains were kept in spore form at -20°C in synthetic medium (SM). *MGCΔ1502-CA_C0764-408s::CT pCLFCA_C0764, MGCΔ1502 pCLFCA_C0764*, *MGCΔ1502 pCLF bcd-etfb-etfa* and *MGCΔ1502 pCons2-1* strains were kept on glucose SM plates with thiamphenicol (10 μg/mL) and directly used to inoculate liquid flask cultures containing glucose SM with thiamphenicol (50 μg/mL). The liquid flask cultures of all *C. acetobutylicum* strains were grown anaerobically at 37°C in 30 mL of SM as previously described (7) with 60 g/L glucose.

Analytical procedures:

The cell concentration was measured turbidimetrically by monitoring the optical density (OD) at 620 nm; an experimentally derived correlation factor of 0.3 g cellular dry weight per $OD_{620\ nm}$ was used for the biomass concentration calculations. Glucose, pyruvate, lactate, acetate, butyrate, acetoin, glycerol, ethanol, acetone and butanol concentrations were measured in the culture supernatants using high-performance liquid chromatography (HPLC) analysis (Agilent 1200 series, Massy, France) as previously described (17).

Enzyme assays:

Ferredoxin-NAD(P)$^+$ reductase activity and NADPH-ferredoxin reductase activity assays:

All enzyme assays were performed in an anaerobic workstation under a nitrogen atmosphere. All reagent solutions were prepared in assay buffer (previously boiled and degassed with nitrogen) and kept under a nitrogen atmosphere. Specific activities were determined in a range where linearity with protein concentration was established. Each enzyme assay was

done at least in duplicate. One unit of enzyme activity is defined as the amount of enzyme that catalyzes the conversion of 1 µmol of substrate per min. The concentrations of components in the reaction mixtures (1 mL of total volume) are given below.

In vitro ferredoxin-NAD(P)$^+$ reductase activity was assayed by measuring the reduction of NAD^+ or $NADP^+$ using electrons from reduced ferredoxin (*CA_C0303*) with H_2 as the reductant of ferredoxin (*CA_C0303*) (31) in the presence of Fe-Fe hydrogenase from *Clostridium acetobutylicum* (*CA_C0028*) (32). Ferredoxin (*CA_C0303*) was purified in the laboratory as previously described (32). The reaction was performed anaerobically at 37°C in 100 mM Tris-HCl buffer (pH 7) with 2 mM DTT, 25 µM FAD, 13 µM ferredoxin or 150 µM methyl viologen, 1,6 mM NAD^+ or $NADP^+$, 6 U (or more) of purified hydrogenase HydA from *C. acetobutylicum* and crude extract (or purified protein), followed by monitoring the increase in $A_{340\ nm}$ as an indication of the appearance of NADH or NADPH using a spectrophotometer (Hewlett Packard 8453). After a gentle stream with hydrogen in the quartz cuvette cells, assays were initiated by the addition of ferredoxin and then, after the reduction of ferredoxin (approximately 5 min), by the addition of NAD^+ or $NADP^+$. In all reactions, nonenzymatic rates were subtracted from the observed initial reaction rates.

In vitro NADPH-ferredoxin reductase activity was assayed by monitoring the increase in $A_{560\ nm}$ as an indication of the reduction of methyl viologen using a spectrophotometer (Hewlett Packard 8453). The reaction was carried out anaerobically at 37°C in quartz cuvette cells in 100 mM Tris-HCl buffer (pH 7,6) with 2 mM DTT, 10 µM FAD, 250 µM NADPH, ethanol 3% vol/vol, 45 U Adh (*S. cerevisiae*), 10 mM methyl viologen, and crude extract or purified protein. Assays were initiated by the addition of methyl viologen. In all reactions, nonenzymatic rates were subtracted from the observed initial reaction rates.

The extinction coefficients of methyl viologen at 560 nm and of NADH and NADPH at 340 nm were 7.71 mM^{-1} cm^{-1}, 6.22 mM^{-1} cm^{-1} and 6.29 mM^{-1} $cm^{-1,}$ respectively. The total protein concentration of the cell-free extract or purified fraction was determined using the Bradford method (Bio-Rad reagent) (33) with bovine serum albumin as the standard.

Purification of the ferredoxin-NAD^+ and ferredoxin-$NADP^+$ reductases in *C. acetobutylicum* under solventogenic conditions:

The *C. acetobutylicum* ATCC 824 strain was kept in spore form at -20°C in SM. The flask cultures of *C. acetobutylicum* strains were grown anaerobically in SM, inoculated with a spore stock at 10% (v/v), and heat-shocked at 80°C for 15 min. Cells were grown at 37°C to an $OD_{620\ nm}$ of approximately 2.0, and the pH was maintained by buffering the culture medium with calcium carbonate prior to inoculation of the bioreactor at 10% (v/v). pH-controlled batch fermentations were performed in SM. A 2 L Biostat B bioreactor (Sartorius, Aubagne, France) was used with a working volume of 1.3 L (34). After sterilization, the medium was sparged with O_2-free nitrogen for 30 min. During the course of the experiment, the medium was maintained under a slight nitrogen overpressure to avoid O_2 entry into the reactor. All tubing was made of butyl rubber, and the reactor gas outlet was protected with a pyrogallol arrangement. Cultures were stirred at 300 rpm, the temperature was set at 35°C, and the pH was maintained at 4.8 with the automatic addition of NH_4OH (3N). The cell concentration was measured turbidimetrically by monitoring the optical density (OD) at 620 nm (Biochrom libra S11), and product formation was measured in duplicate using HPLC analysis (Agilent 1200 series, Massy, France) (17). When the $OD_{620\ nm}$ reached approximately 16, after the switch from the acidogenic to solventogenic phase, cells were harvested under hydrogen pressure and transferred into an anaerobic chamber. The cells were washed and concentrated 20 times in 100 mM Tris-HCl 2 mM DTT 10% glycerol (pH 7.6) buffer and frozen at -80°C.

All purification procedures were performed under anaerobic conditions. All purification buffers were degassed in advance, and 10 μM FAD and 2 mM DTT were added to prevent nonreversible activity losses.

Frozen cells from solventogenic batch cultures of *C. acetobutylicum ATCC 824* were thawed and broken by sonication using an ultrasonic disintegrator (Vibracell 72434, Bioblock) at 4°C in four cycles of 30 s at 2-min intervals. Debris was removed by centrifugation at 8600 ×g for 10 min at 4°C (Sigma centrifuge 2-16K). Nucleic acids were precipitated by the addition of streptomycin sulfate (200 μg/mL) to the supernatant and removed by centrifugation as described above. The recovered extract was then diluted 5 times in 100 mM Tris-HCl buffer (pH 8) before loading on a 5 mL HiTrap Capto DEAE matrix (GE Healthcare, ref. 28-9165-40) connected to an AKTA purifier (GE Healthcare, Sweden). Active fractions were screened with the ferredoxin NAD^+ and ferredoxin $NADP^+$ reductase assay using ferredoxin as previously described. The column was equilibrated in 100 mM Tris-HCl buffer (pH 8), and elution was performed with a 3-step gradient of 100 mM Tris-HCl + 1 M NaCl buffer (pH 8): 1 CV 0–4%, 20 CV 4–16% (target elution) and 5 CV 16–100%; 2 mL fractions were collected. For ferredoxin-$NADP^+$ reductase activity, the most active fractions from the Capto DEAE column were pooled before being loaded on a Resource Q column equilibrated in 100 mM Tris-HCl buffer (pH 8) for a second chromatographic step. The most active eluted fractions were then collected and concentrated on a Vivaspin 15/10000 MW (Sartorius Stedim, ref. VS1502) to reduce the sample volume to 150 μL by centrifugation at 3000 ×g for 15 min. For the last purification step, a 150 μL sample volume was loaded on a Superose 12, 10/300 GL column (GE Healthcare, ref. 17-5173-01) previously equilibrated in 100 mM Tris-HCl + 150 mM NaCl buffer (pH 7.6), and 400 μL fractions were collected. For ferredoxin-NAD^+ reductase activity, the active fractions from the Capto-DEAE column from each eluted peak were pooled before being loaded onto a

Resource Q equilibrated in 100 mM Tris-HCl buffer (pH 8) for a second chromatographic step or onto a Superose 12 10/300 GL column (GE Healthcare, ref. 17-5173-01) previously equilibrated in 100 mM Tris-HCl + 150 mM NaCl buffer (pH 7.6), and 400 µL fractions were collected. Finally, the total protein concentration of the cell-free extract or purified fractions was determined using the Bradford method (Bio-Rad reagent) (31) with bovine serum albumin as the standard.

The yields and purification factor of each step were calculated. The purity factor of the separate active fractions was also evaluated using SDS electrophoresis in 40 mL polyacrylamide gels.

Identification of the gene coding for ferredoxin-NAD$^+$ and ferredoxin-NADP$^+$ reductase activities:

Active eluted fractions collected after Superose 12 or Resource Q chromatography were loaded onto denaturing gel electrophoresis, and proteins were silver stained. For the ferredoxin-NADP$^+$ reductase active fraction, the region of the gel corresponding to the protein at 45 kDa was used, and for the ferredoxin-NAD$^+$ reductase active fractions, the regions of the gel corresponding to the proteins at i) 41, 37, and 34 kDa and ii) at 167 and 53 KDa were used. The gel regions were cut out using a sterile pipette tip. The gel plugs were then used for the identification of proteins by mass spectrometry. Each sample was subjected to trypsin digestion and analyzed by *nano-LC–MS/MS* on a CapLC-Q-TOF2 (Waters) and by MALDI on a MALDI MX (Waters). The candidate proteins were identified with ProteinLynx Global Server (Waters) and Mascot (Matrix Science) software using the Protein Data Bank entry for *C. acetobutylicum*. In both analyses, for ferredoxin-NADP$^+$ reductase activity, only one protein was identified with a significant score (77% sequence coverage). For ferredoxin NAD$^+$

reductase activity, four proteins were identified with significant scores: a) butyryl-CoA dehydrogenase, 58.6% sequence coverage; b) EtfB, 78.4% sequence coverage; c) GltA, 78.4% sequence coverage, and d) GltB, 50.7% sequence coverage.

Purification of CAC0764 and Bcd-EtfB-EtfA fused with a Strep-tag:

CAC0764 protein and Bcd-EtfB-CST-EtfA complex protein were produced and purified in the form of Strep-tag II fused proteins as described previously by Gauquelin *et al*. 2018 (30), with the following modifications: sodium dithionite was not added to the elution buffer, and 25 μM FAD was added to all buffers.

References:

1. Jones D T. Applied acetone-butanol fermentation, p 125–168. In Bahl H, Dürre P (ed), Clostridia: biotechnology and medical applications. Wiley-VCH Verlag GmbH, Weinheim, Germany (2001).

2. Jones D.T. & Woods D.R. Acetone-butanol fermentation revisited. *Microbiol Res* **50:**484–524 (1986).

3. Jones DT, Van der Westhuizen A, Long S, Allcock ER, Reid SJ, & Woods DR. Solvent production and morphological changes in *Clostridium acetobutylicum*. *Appl Environ Microbiol* **43:**1434–1439 (1982).

4. Durre P. Biobutanol: an attractive biofuel. *Biotechnol. J.* 2, 1525-1534 (2007).

5. Ni Y, & Sun Z. Recent progress on industrial fermentative production of acetone-butanol-ethanol by *Clostridium acetobutylicum* in China. *Appl Microbiol Biotechnol* **83:**415–423. http://dx.doi.org/10.1007/s00253-009-2003-y (2009)

6. Vasconcelos I, Girbal L, & Soucaille P. Regulation of carbon and electron flow in *Clostridium acetobutylicum* grown in chemostat culture at neutral pH on mixtures of glucose and glycerol. *J Bacteriol* 176**:** 1443–1450 (1994).

7. Girbal L, & Soucaille P. Regulation of *Clostridium acetobutylicum* metabolism as revealed by mixed-substrate steady-state continuous cultures: role of NADH/NAD ratio and ATP pool. *J Bacteriol* **176:** 6433–6438 (1994).

8. Girbal L, Vasconcelos I, Saint-Amans S, & Soucaille P. How neutral red modified carbon and electron flow in *Clostridium acetobutylicum* grown in chemostat culture at neutral pH. *FEMS Microbiol Rev* **16:**151–162. http://dx.doi.org/10.1111/j.1574-6976.1995.tb00163.x (1995).

9. Girbal L, Croux C, Vasconcelos I, & Soucaille P. Regulation of metabolic shifts in *Clostridium acetobutylicum* ATCC 824. *FEMS Microbiol Rev* **1 7 :**287–297. http://dx.doi.org/10.1111/j.1574-6976.1995.tb00212.x (1995).

10. Girbal L, & Soucaille P. Regulation of solvent production in *Clostridium acetobutylicum*. Trends Biotechnol **16:**11–16. http://dx.doi.org/10.1016/S0167-7799(97)01141-4 (1998).

11. Wiesenborn DP, Rudolph FB, & Papoutsakis ET. Phosphotransbutyrylase from *Clostridium acetobutylicum* ATCC 824 and its role in acidogenesis. *Appl Environ Microbiol* **55:**317–322 (1989a).

12. Wiesenborn DP, Rudolph FB, & Papoutsakis ET. Coenzyme A transferase from *Clostridium acetobutylicum* ATCC 824 and its role in the uptake of acids. *Appl Environ Microbiol* **55:**323–329 (1989b).

13. Sauer U, & Dürre P. Differential induction of genes related to solvent formation during the shift from acidogenesis to solventogenesis in continuous culture of *Clostridium acetobutylicum*. *FEMS Microbiol Lett* **125:** 115–120. http://dx.doi.org/10.1111/j.1574-6968.1995.tb07344.x (1995).

14. Soni B.K., Soucaille P. & Goma G. Continuous acetone butanol fermentation: a global approach for the improvement in solvent productivity. Appl. Microbiol. Biotechnol. 25, 317-321 (1987).

15. Soni B.K., Soucaille P. & Goma G. Continuous acetone-butanol fermentation: influence of vitamins on the metabolic activity of *Clostridium acetobutylicum*. Appl. Microbiol. Biotechnol. 27, 1-5 (1987).

16.Jang YS , J.Y. Lee, J. Lee, J.H. Park, J.A. Im, M.H. Eom, J. Lee, S.H. Lee, H. Song, J.H. Cho, Y,Seung do, & S.Y. Lee, Enhanced butanol production obtained by reinforcing the direct butanol-forming route in *Clostridium acetobutylicum*. *MBio*. **3**, e00314-12 (2012)

17. Dusséaux S, Croux C, Soucaille P, & Meynial-Salles I.. Metabolic engineering of *Clostridium acetobutylicum* ATCC 824 for the high-yield production of a biofuel composed of an isopropanol/butanol/ethanol mixture. *Metab. Eng*., 18,1-8 (2013).

18. Nguyen N P T, Raynaud C., Meynial-Salles I. & Soucaiille P. Reviving the weizmann process for commercial n-butanol production, *Nature communications*, 9, 3682 (2018).

19. Yoo M, Bestel-Corre G, Croux C, Riviere A, Meynial-Salles I, & Soucaille P. A quantitative system-scale characterization of the metabolism of *Clostridium acetobutylicum*. *MBio* 2015;6(6):e01808–15 (2015)

20. Petitdemange H. Cherrier C; Raval G. & Gayn R. Regulation of the NADH and NADPH ferredoxin oxidoreductase in Clostridia of the butyric group, *Biochimica et Biophysica Acta,* 421, 334-347 (1976).

21. Lee J. Yun H., Feist A., Palsson B. & Lee S. Y. Genome-scale reconstruction and in silico analysis of the *Clostridium acetobutylicum* ATCC824 metabolic network. *Appl Microbiol. Biotechnol.* 80, 849-862 (2008).

22. Ceccarelli E. A., Arakaki A. K., Cortez N. &Carrillo N.. Functional plasticity and catalytic efficiency in plant and bacterial ferredoxin- NADP(H) reductases *Biochem Biophys. Acta*, 155-165 (2004).

23. Muller V., Chowdhury N. P. & Basen M. Electron bifurcation: a long-hidden energy-coupling mechanism: Annu. Rev. Microbiol., 72, 331-353 (2018).

24. Liang J., Huang H., & Wang S. Distribution, Evolution, Catalytic Mechanism and Physiological Functions of the Flavin-based electron-bifurcating NADH-dependent reduced ferredoxin:NADP+ oxidoreductase: Frontiers in Microbiology, 1-12 (2019).

25. Lo J., Zheng T., Olson D. G., Ruppertsberer N., Tripathi S.A., Guss A.M. and Lynd L. R. Deletion of nfnAB in *Thermoanaerobacterium saccharolyticum* and its effect on metabolism: *J. Bacteriol.,* 197, 2920-2929 (2015).

26. Crown S.B., Indurthi D.C., Ahn W.S., Choi J., Papoutsakis E.T., & Antoniewicz M.R. Resolving the TCA cycle and pentose-phosphate pathway of *Clostridium acetobutylicum* ATCC 824: Isotopomer analysis, in vitro activities and expression analysis., *Biotechnol. J.,* 6 300-305 (2011).

27. Heap JT, Pennington OJ, Cartman ST, Carter GP, & Minton NP. The ClosTron: a universal gene knock-out system for the genus *Clostridium. J Microbiol Methods*. 70:452-64 (2007)

28.Croux C, Nguyen NPT, Lee J., Raynaud C. Saint Prix F., Gonzales Pajuelo M. , Meynial-Salles I. & Soucaille P. Construction of a restriction-less, marker-less mutant useful for functional genomic and metabolic engineering of the biofuel producer *Clostridium acetobutylicum*. *Biotechnol. Biofuels*. **9**, 23 (2016).

29. Jones S.W., Paredes C.J., Tracy B., Cheng N., Sillers R., Senger R.S., & Papoutsakis E.T. The transcriptional program underlying the physiology of clostridial sporulation, *Genome Biol*. 9, R114 (2008)

30 Papoutsakis E. T. Equations and calculations for fermentations of butyric acid bacteria: *Biotech Bioeng*, 174-187 (1983)..

31. Demuez M., Cournac L., Guerrini O., Soucaille P., Girbal . Complete activity profile of Clostridium acetobutylicum [FeFe]-hydrogenase and kinetic parameters for endogenous redox partners, *FEMS Microbiol. Lett*. 275, 113–121 (2007)

32. Gauquelin C, Baffert C, Richaud P, Kamionka E, Etienne E, Guieysse D, Girbal L, Fourmond V, André I, Guigliarelli B, Léger C, Soucaille P, Meynial-Salles I. Roles of the F-domain in [FeFe] hydrogenase *Biochim Biophys Acta*. *Bioenergetics*, 1859:69-77 (2018)

33. Bradford M. A rapid and sensitive method fort the quantification of microgram quantities of protein utilizing the principle of protein–dye binding. *Anal. Biochem*.72, 248–254 (1976)

34. Meynial-Salles I.*, Gonzalez-Pajuelo M.*, Mendes P., Andrade J. C., Vasconcelos I. & Soucaille P. Metabolic engineering of *Clostridium acetobutylicum* for the industrial production of 1.3 propanediol from glycerol: *Metabolic Eng*., 7, 329-336 (2005). * equivalent contribution.

Acknowledgments:

This work was financially supported by the Agence Nationale de la Recherche (Grants ANR acetoH2 PNRB 2006 ANR Bio6 BioE-001, Biobutafuel ANR 088 BioE-012-01, Cellutanol ANR 14 CE05-0019-02) and by the BIOCORE European Project (Grant no. FP7-241566). The authors

thank AJE for English language editing of the document (certification code 3DBE-123F-E411-E361-B16P).

Author contributions:
CF, AR, MH, SDR, CP, MP, and SD designed and performed the experiments. LG participated in the conception of this study. PS and IMS conceived this study, analyzed the data, discussed the results and wrote the manuscript.

Additional information:
Supplementary information accompanies this paper.

Competing interests:
A patent application has been filed related to this work.

Supporting information:

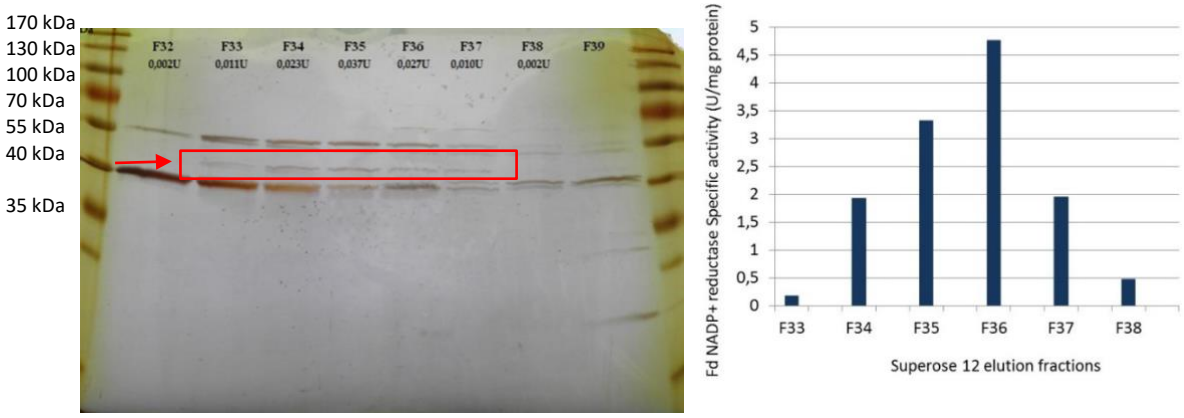

A **B**

Supplementary Fig. 1: a) SDS-PAGE analysis of active eluted fractions collected after Superose 12 chromatographic separation (proteins were silver stained). b) Ferredoxin-NADP⁺ reductase activity of the corresponding fractions.

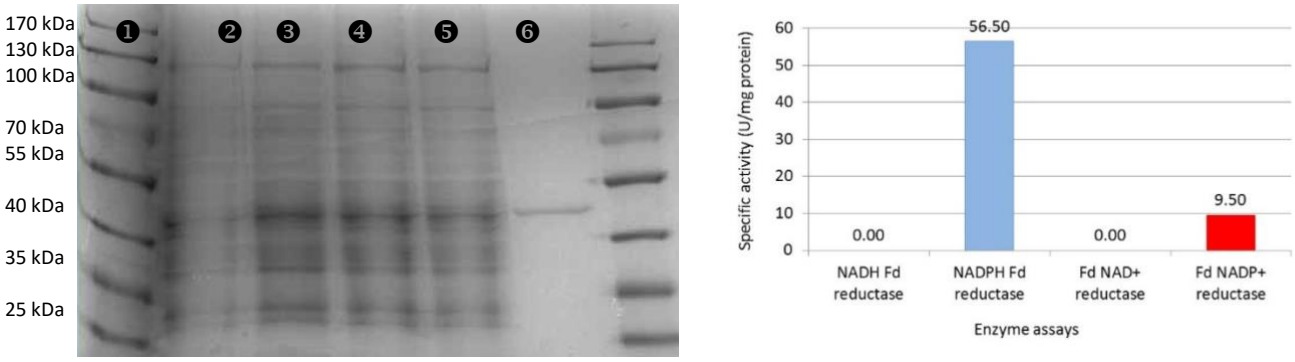

A B

Supplementary Fig. 2: A) SDS-PAGE of purified CAC0764-Strep-tag 1) protein ladder 2) cell-free extract 3) streptomycin sulfate treatment 4) avidin treatment 5) loaded sample 6) active eluted fraction. B) Enzymatic activities of the CAC0764-Strep-tag protein determined using methyl viologen (blue) or reduced ferredoxin (red).

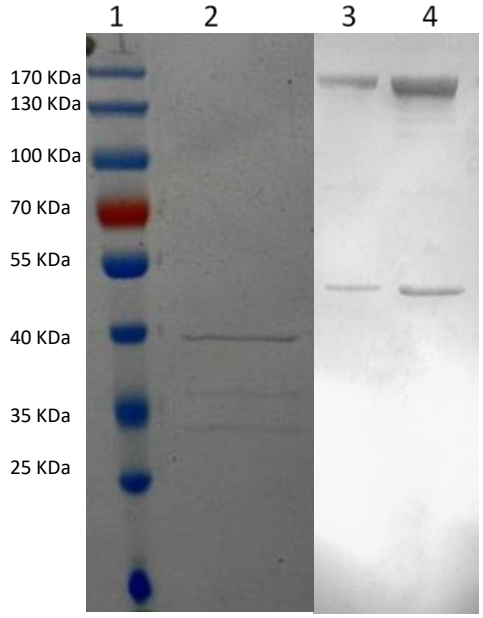

Supplementary Fig. 3: Silver-stained SDS-PAGE of the 1) protein ladder , 2) active eluted fractions from Resource Q, and 3-4) active eluted fraction from gel filtration.

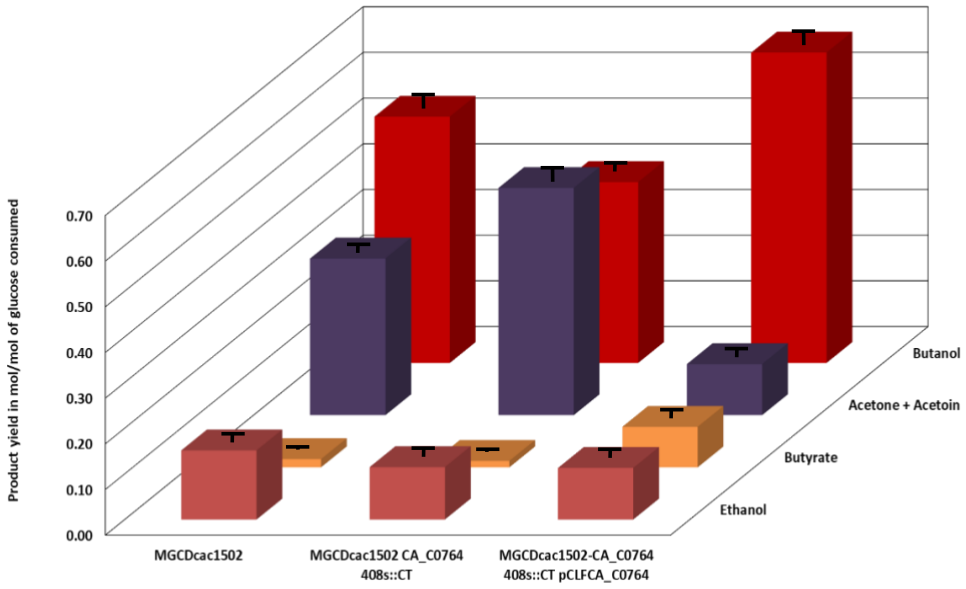

Supplementary Fig. 4: Comparative final product yields in mol/mol of glucose consumed for the three *C. acetobutylicum* strains: *MGCΔcac1502, MGCΔcac1502-CA_C0764-408s::CT, MGCΔcac1502-CA_C0764-408s::CT (pCLFCA_C0764).*

Supplementary Table 1: List of strains and plasmids used in this study.

Strains/Plasmids	Relevant characterictics*	Source
C. acetobutylicum		
ATCC 824	Wild type	ATCC
MGC*Δ1502*	ΔCA_C1502	Croux *et al*. 2016
MGC*Δ1502 pCons2-1*	ΔCA_C1502	Croux *et al*. 2016
MGC*Δ1502-CA_C0764-408s::CT*	MGC*Δ1502 CA_C0764* mutant	This study
MGC*Δ1502-CA_C0764-408s::CT pCLFCA_C0764*	complemented MGC*Δ1502 CA_C0764* mutant	This study
MGC*Δ1502 pCLFCA_C0764*	overexpression of *CA_C0467* gene from the pCLF942 plasmid	This study
MGC*Δ1502-gltB181s::CT*	MGC*Δ1502 gltB* mutant	This study
MGC*Δ1502 pCLF bcd-etfB-etfA*	overexpression of *bcd-etfb-etfA* genes from the pCLF942 plasmid	This study
E. coli		
TOP10		Invitrogen
Plasmids		
pThl_HydA-LL-Ctag	MLS^r; AP^r; *repL*; *hydA* with hydA promoter and adc terminator	Caserta *et al*. 2018
pCST-LL-CA_C0764	pPH_HydA-LL-Ctag derivative with *CA-C0764* insertion and pPH replacement with pthl	This study
pCST-LL-etfb-etfA	pPH_HydA-LL-Ctag derivative with etfb and etfa insertion and pPH replacement with pthl	Yoo et *al. 2015*
pCST-LL-bcd-etfb-etfa	pCST-LL-etfBetfA derivative with bcd insertion	Yoo *et al.* 2015
pSOS94	MLS^r ; AP^r ; repL ; ctfA ; ctfB ; adc with ptb promoter and adc terminator	GenBank: AY187685.1
pCLF1	Cm^r ; repL ; flp1	Croux *et al*. 2016
pCLF *CA_C0764*	pCLF1 derivative with *CA_C0764* with *ptb* promoter and *adc* terminator	This study
pCLF bcd-etfb-etfa	pCLF1 derivative with *bcd-etfb-etfa* with *ptb* promoter and *adc* terminator	This study
pMTL007		Heap *et al.* 2007
pMTL007::cac-CA_C0764-408s	ClosTron plasmid retargeted to *C. acetobutylicum CA_C0764* gene	This study
pMTL007::cac-gltB181s	ClosTron plasmid retargeted to *C. acetobutylicum gltB* gene	This study
pMTL007::cac-CA-C2710-159s	ClosTron plasmid retargeted to *C. acetobutylicum CA_C2710* gene	This study
pMTL007::cac-CA-C2710-101as	ClosTron plasmid retargeted to *C. acetobutylicum CA_C2710* gene	This study

***abbreviations: MLS^r: macrolide, lincosamide, Streptogramin B resistance; Ap^r: ampicillin resistance; catP: thiamphenicol resistance**

Supplementary Table 2: List of primers used in this study.	
Name	Oligonucleotide sequences
408/409s-IBS	AAAAAAGCTTATAATTATCCTTAGGCTACAATGTTGTGCGCCCAGATAGGGTG
408/409s-EBS1d	CAGATTGTACAAATGTGGTGATAACAGATAAGTCAATGTTACTAACTTACCTTTCTTTGT
408/409s-EBS2	TGAACGCAAGTTTCTAATTTCGATTTAGCCTCGATAGAGGAAAGTGTCT
cac0764del_for	cgagccaataaaatttcacgagata
cac0764del_rv	ccaacctctataagtctttcttcaagctta
Ocac0764f	AGGATCCATCAAAATTTAGGAGGTTAGTTA
Ocac0764r	GGCGCCTTAATTATTCTTGCAATACTCATCAATAGTTTC
ESB universal	gtttactgaacgcaagtttctaatttcg
ErmB3'- R- F	cgccaaagtaaacaatttaagtaccgttac
fabZf	TCCAAGTATAGGCTTCTTTCCC
fabZr	GGTCATTACCCAGGTAAACCA
gapCf	CACATTAGATGGTCCACACAGAA
gapCr	AGCTAAGTCAGGAATAACTTGGC
gapNf	GGTTCTTGAGCTTGGTGGTAAA
gapNr	TTTACAGCAGTACACCTTTGGC
ccac0764BAMf	aattggatccatcaaaatttaggaggttagttagaatggataaccctaatttattgtcagaag
ccac0764SMAr	aattcccgggattattcttgcaatactcatcaatagtttc
CAC2710-101asIBS	aagcttataattatccttaccttcccttatagtgcgcccagatagggtg
CAC2710-159sIBS	gcacttgaggaagtgcgcccagatagggtg
CAC2710-159sEBS1d	acaaagaaaggtaagttagcttcctcgacttatctgttatcaccacatttgtacaatctg
RBS nat bcd_rec for	AAATGAGCACGTTAATCATTTAACATAGATAATTGGATCCAGGAGGTAAGTTTATATGGATTTTAATTTAACAAG
etfa_rec_rev	AGAAACAATCTCTTTTACTGGCAAATCATTAAGTGGCGCCTTAATTATTAGCAGCTTTAACTTGAGCTATTAA
pCLF prom seq_for	AACACCACGTAGTTATTGGGAGG
pCLF term_rev	CTGCAAGAATGTGAGAGCTAG
psos prom univ	cttttggtcgtagagcacacgg
pSOSterm	ccgctcacaattccacacaacatacg
gltB_direct181S	GCTGCAGTTAATATGTAAGGGGGCGG
gltB_reverse181S	CCTTTGGAATCTTAGGCTTTACCCATCC

Supplementary material:

All of the chemicals were of reagent grade. Coenzymes such as methyl viologen, acetoacetyl-CoA, NAD(P)H and NAD(P^+) were purchased from Sigma Chimie (St. Quentin Fallavier, France).

All gases used (carbon monoxide, nitrogen and a mixture of carbon monoxide, hydrogen and nitrogen) were of the highest purity available and were purchased from Air Liquid (Paris, France). DNA restriction enzymes, Antarctic phosphatase enzyme and T4 DNA ligase were obtained from New England Biolabs (Evry, France) and used according to the manufacturer's instructions. The proofreading Phusion DNA polymerase (New England Bioloabs) was used for PCR amplification prior to vector construction, and *One taq* DNA polymerase (New England Biolabs) was used for routine, control PCR amplifications. TOPO cloning was performed with the Zero Blunt TOPO Cloning Kit for sequencing as recommended by the manufacturer's instructions, and homologous cloning was performed with the GeneArt® Seamless Cloning & Assembly Kit following the manufacturer's instructions (Thermo Fisher Scientific, Saint Aubin, France).

Supplementary method 1: plasmid construction
1-Construction of *pMTL007*::cac-*CA_C0764*-408s:

The intron target site was identified at bp 408/409 (from the start of the ORF) on the sense strand, and the intron retargeting PCR primers 408/409-IBS, 408/409-IEBS1d, and 408/409-EBS2 (Supplementary Table 2) were designed using a computer algorithm (1). The three primer sets 408/409-IBS, 408/409-IEBS1d, 408/409-EBS2 and the EBS universal primers were used in a single-tube reaction with the pMTL007 plasmid (2) to mutate the intron at several positions spanning a 350 bp region. PCR designed to retarget the intron by primer-mediated mutation was performed according to the protocol of the Targetron Gene Knockout System Kit (http://www.sigmaaldrich.com/life-science/functional-genomics-and-rnai/targetron.html). The 350 bp PCR fragment was purified and then cloned into the pMTL007 plasmid at the HindIII and BsrGI sites to replace the original intron fragment. The ligation product was then introduced into Top10 chemically competent *E. coli* cells

(Invitrogen™). Single colonies were then grown in LB liquid culture supplemented with ampicillin (100 µg/mL) overnight at 37°C to finally carry out DNA plasmid extraction (GenElute HP plasmid miniprep kit, Sigma) and check for the presence of the *pMTL007::cac-CA_0764-408s* plasmid. The retargeted *pMTL007::cac-CA_0764-408s* plasmid was finally controlled by restriction and by DNA sequencing using the 408/409-IBS and 408/409-IEBS1d primers (Supplementary Table 2).

2-Construction of *pMTL007Ca::gltB-180s*: A similar method was applied to generate the intron-retargeted *pMTL007Ca::gltB-180s* plasmid. The intron target site was identified at 181/182 bp on the sense strand using the Perutka algorithm (1).

3-Construction of *pMTL007Cs::2710-101as* and *pMTL007Cs::2710-159s:* As previously described, the Perutka algorithm (1) was used to identify the intron target site. Two positions, 101/102 on the antisense strand and 159/160 on the sense strand, were selected.

4-Construction of *pCLF-CA_C0764:*

The *CA_C0764* gene was amplified from the genomic DNA of *C. acetobutylicum ATCC824* using the Ocac0764f and Ocac0764r primers (Supplementary Table 2). The primers were designed to introduce an RBS region along with the *CA_C0764* gene, as well as placing BamHI and SfoI restriction sites upstream and downstream, respectively. The amplified PCR fragment was then subcloned into a Zero Blunt TOPO vector (Invitrogen, Saint Aubin, France) to yield the Zero Blunt TOPO–*CA_C0764* plasmid, and the product was sequenced using universal primers T7P and T3P to assure that no mutations were introduced. The fragment containing the *CA_C0764* gene was purified on an agarose gel after digestion of the Zero Blunt TOPO–*cac0764* vector with BamHI and SfoI. The 7 kb pSOS94 vector (3) was also digested with BamHI and SfoI and ligated to the BamHI-SfoI digested *sadh* gene, yielding the 6.25 kb pSOS94-CA-C0764 vector. The *pSOS94-CA_C0764* vector was digested with SalI, and the operon-

containing fragments from each vector were purified on an agarose gel. The 4.9 kb pCLF1 vector (4) was digested with SalI, treated with Antarctic phosphatase and ligated with the previously purified fragment to yield *pCLF-CA_C0764*.

5.-Construction of *pCLF-bcd-etfb-etfa:*

The *bcd-etfb-etfa* operon was amplified from the genomic DNA of *C. acetobutylicum MGC⊿cac1502* using the *RBS nat bcd_rec_for* and *etfa_rec_rev* primers (Supplementary Table 2). The primers were designed to introduce the native bcd RBS along with the operon and *pCLF-CA_C0764* homologous regions. The purified PCR product was directly ligated with *pCLF-CA_C0764* previously digested with ScaI et SfoI and purified using the GeneArt® Seamless Cloning & Assembly Kit. The *pCLF-bcd-etfb-etfa* plasmid was controlled by PCR using the primers *pCLF prom seq_for* and *pCLF term_rev* (Supplementary Table 2), by restriction profiling, and finally by promoter-*bcd-etfb-etfa*-terminator region resequencing.

6-Construction of the *pCST-LL-CA_C0764:*

The *CA_C0764* gene was amplified from the genomic DNA of *C. acetobutylicum ATCC824* using *ccac0764BAMf* and *ccac0764SMAr* primers (Supplementary Table 2). The primers were designed to introduce an RBS region along with the *CA_C0764* gene, as well as placing BamHI and SmaI restriction sites upstream and downstream, respectively. The purified PCR product was further ligated with the product digested with BamHI and SmaI and purified *pthlA-CaHydA-LL-C-Tag* plasmid (5), yielding the *pCST-LL-CAC0764* vector. The *pCST-LL-CAC0764* vector was checked by PCR using *pSOSprom_univ* and *pSOSterm* primers (Supplementary Table 2), by restriction profiling, and finally by promoter-*CAC_O764-CST*-terminator region resequencing.

Supplementary method 3: Transformation procedures:

E. coli Top10 (Invitrogen) was transformed using heat shock (30 s at 42°C) following the manufacturer's instructions.

MGC*Δcac1502* was electroporated as previously described (6), except that unmethylated DNA was used because the *cac1502* gene encoding the type II restriction endonuclease Cac824I was deleted (4). For transformation with the retargeted *pMTL007::cac-CA_C0764-408s,* after 5 hours of recovery, cells were plated on RCA (Clostridium Nutrient Medium with 15 g/L agar and Fluka (Saint-Quentin Fallavier, France, n°27546) medium supplemented with thiamphenicol (10 μg/mL)). Single colonies were chosen from the plate and streaked separately on an RCA plate with erythromycin (40 μg/ml) to select integrants. The insertion mutants were screened via colony PCR using the primers cac0764del_for and cac0764del_rv (Supplementary Table 2) flanking the target site. The PCR products were purified and confirmed by DNA sequencing. One of the colonies was selected to cure the *pMTL007::cac-CA_C0764-408s* plasmid and generate *MGCΔcac1502CA_C0764*-408s::CT. This clone was inoculated into Clostridum Growth Medium (CGM) supplemented with erythromycin (40 μg/mL) for successive subcultures, as previously described (3). One hundred microliters of fully grown culture was inoculated into 1 mL of fresh CGM supplemented with erythromycin (40 μg/mL) and grown anaerobically at 37°C for at least 12 hours until full growth was achieved. This transfer process was repeated at least 3 times. The last culture was then plated onto a solid RCA plate supplemented with erythromycin (40 μg/mL). Colonies were restreaked successively onto RCA plates supplemented with thiamphenicol (10 μg/mL) and then onto RCA plates supplemented with erythromycin (40 μg/mL). One erythromycin–resistant and thiamphenicol-sensitive clone was selected and inoculated into 3 mL of SM (7) supplemented with erythromycin (40 μg/mL), grown anaerobically at 37°C for at least 24 hours and

transferred to 30 mL of SM supplemented with erythromycin (40 μg/mL). The culture was grown anaerobically at 37°C for 7 days until sporulation, and then the spore suspension was stored at –20°C. Southern hybridization was finally used to validate the presence of a single-intron insertion into the genome of *MGCΔcac1502CA_C0764-408s::CT*.

A similar approach was applied to yield the *MGCΔcac1502-gltB181s::CT* strain. The insertion mutants were screened using the primers *gltB181s direct* and *gltB181s reverse* (Supplementary Table 2) flanking the target site. The PCR products were purified and confirmed by DNA sequencing.

For transformation with *pCLFCA_C0764* and *pCLF-bcd-etfb-efta*, after 5 hours of recovery, cells were plated on RCA medium supplemented with thiamphenicol (10 μg/mL). Single colonies were chosen from the plate and streaked separately on an SM plate with thiamphenicol (10 μg/ml).

For transformation with *pCST-LL-CA_C0764* and *pCST-LLbcd-etfb-efta*, after 5 hours of recovery, cells were plated on RCA medium supplemented with erythromycin (40 μg/ml). Single colonies were chosen from the plate and streaked separately on an SM plate with erythromycin (40 μg/mL).

Supplementary method 4: Southern blot analysis:

Chromosomal DNA (3–6 μg) of both the *MGCΔ1502* and *MGCΔ1502-CA_C0764-408s::CT* strains was digested with the HindIII-HF restriction enzyme and loaded on a 0.8% agarose gel. The transfer was performed in 20xSSC on a nylon membrane. The probe used for hybridization was generated by PCR using ESB universal and ErmB3'- R- F primers (Supplementary Table 2) and then labeled using a DIG High Prime DNA Labeling and Detection Starter Kit II (Roche,

Mannheim Germany). The protocols for hybridization and detection were performed according to the Roche instructions.

Supplementary method 5: RNA isolation, cDNA synthesis and RT-qPCR analysis:

After the activation of spores by heat treatment at 80°C for 15 min, both MGC*Δcac1502 and MGCΔcac1502 cac0764-408s::CT* strains were cultivated in duplicate in 60-mL glass vials under strict anaerobic conditions at 37°C in SM.

When the OD_{620} of *MGCΔcac1502* and *MGCΔcac1502CA_C0764-408s::CT* cultures reached 2.9 and 1.5, respectively, cultures were sampled, immediately frozen in liquid nitrogen and stored at -80°C until use.

Total RNA isolation was performed as previously described (8). Briefly, the frozen sampled cultures were ground promptly in a liquid nitrogen-cooled mortar. RNA was extracted using an RNeasy Midi Kit (Qiagen). Contaminant genomic DNA was then removed using the RNase-Free DNase Set (Qiagen) following the manufacturer's instructions, and the total DNase-treated RNA was then purified and concentrated using an RNA Cleanup Kit (Qiagen). RNA quantification was performed using a NanoDrop ND-1000 spectrophotometer (Labtech France) at 260 nm, and purity was analyzed by determining the 260 nm/280 nm ratio (purity > 2.1). RNA integrity was also verified on RNA 6000 Nano Chips using an Agilent 2100 Bioanalyzer (Agilent Technologies).

For cDNA synthesis, 1 µg of total RNA was used in a 20 µL reverse transcription (RT) reaction mixture containing iScript Reverse-transcriptase and a blend of oligo(dT) and random hexamer primers using the iScriptTM cDNA Synthesis Kit (Bio-Rad) according to the manufacturer's instructions.

Quantitative real-time PCR (qPCR) was conducted with a MyiQ™ Real Time PCR Detection System (Bio-Rad). Each sample was tested in triplicate in a 96-well plate (Bio-Rad). The reaction mix (25 µL final volume) consisted of 12.5 µL of SsoAdvanced Universal SYBR Green Supermix (Bio-Rad), 2.5 µL of the primer pair (200 nM final concentration), 2.5 µL of HO and 5 µL of a 1/10 dilution of the cDNA preparation. The absence of possible genomic DNA contamination was checked in each DNase-treated RNA sample. A blank (no template control) was also incorporated in each assay. The thermocycling program consisted of one hold at 95°C for 30 s, followed by 40 cycles of 10 s at 95°C and 30 s at 57°C. After completion of these cycles, melting-curve data were then collected to verify PCR specificity, contamination and the absence of primer dimers.

The fabZ gene (*CA_C3571*) was chosen as an internal control (9). The primer pairs fabZf/fabZr, gapCf/gapCr and gapNf/gapNr (Supplementary Table 2) were used to amplify the *fabZ*, *gapC* (*CA_C0709*) and *gapN* genes (*CA_C3657*), respectively.

Expression data and associated technical errors were calculated on triplicate experiments using the gene expression module of iQ5 software (Bio-Rad), which uses the model outline on the geNorm website.

References:

1. Perutka J, Wang W, Goerlitz D, & Lambowitz AM Use of computer-designed group II introns to disrupt Escherichia coli DExH/D-box protein and DNA helicase genes. J. Mol. Biol. 336:421-39 (2004).

2. Heap JT, Pennington OJ, Cartman ST, Carter GP, & Minton NP. The ClosTron: a universal gene knock-out system for the genus Clostridium. *J Microbiol Methods*. 70:452-64 (2007)

3. Dusséaux S, Croux C, Soucaille P, & Meynial-Salles I. Metabolic engineering of *Clostridium acetobutylicum* ATCC 824 for the high-yield production of a biofuel composed of an isopropanol/butanol/ethanol mixture. *Metab. Eng*., 18,1-8 (2013).

4.Croux C, Nguyen NPT, Lee J., Raynaud C. Saint Prix F., Gonzales Pajuelo M., Meynial-Salles I. & Soucaille P. Construction of a restriction-less, marker-less mutant useful for functional genomic and metabolic engineering of the biofuel producer Clostridium acetobutylicum. *Biotechnol. Biofuels*. **9**, 23 (2016).

5. Caserta, G., Papini, Adamska-Venkatesh, A., Pecqueur, L., Sommer, C., Reijerse, E., Lubitz, W., Gauquelin, C., Meynial Salles I., Pramanik, D., Artero, Atta, del Barrio, M., Faivre, Fourmond, Léger, & Fontecave, M. Engineering an [FeFe]-Hydrogenase: Do Accessory Clusters Influence O2 Resistance and Catalytic Bias ? *J. Am. Chem. Soc., 140* (16), 5516-5526 (2018).

6. Mermelstein, L.D., Welker, N.E., Bennett, G.G., & Papoutsakis, E.T**.,** Expression of cloned homologous fermentative genes in *Clostridium acetobutylicum* ATCC 824. Biotechnology. 10, 190-195 (1992).

7. Girbal L, & Soucaille P. Regulation of *Clostridium acetobutylicum* metabolism as revealed by mixed-substrate steady-state continuous cultures: role of NADH/NAD ratio and ATP pool. *J Bacteriol* **176:** 6433–6438 (1994).

8. Yoo M, Bestel-Corre G, Croux C, Riviere A, Meynial-Salles I, & Soucaille P. A quantitative system-scale characterization of the metabolism of *Clostridium acetobutylicum*. *MBio*;6(6):e01808–15 (2015)

9. Jones S.W., Paredes C.J., Tracy B., Cheng N., Sillers R., Senger R.S., & Papoutsakis E.T. The transcriptional program underlying the physiology of clostridial sporulation, *Genome Biol*. 9, R114 (2008)